



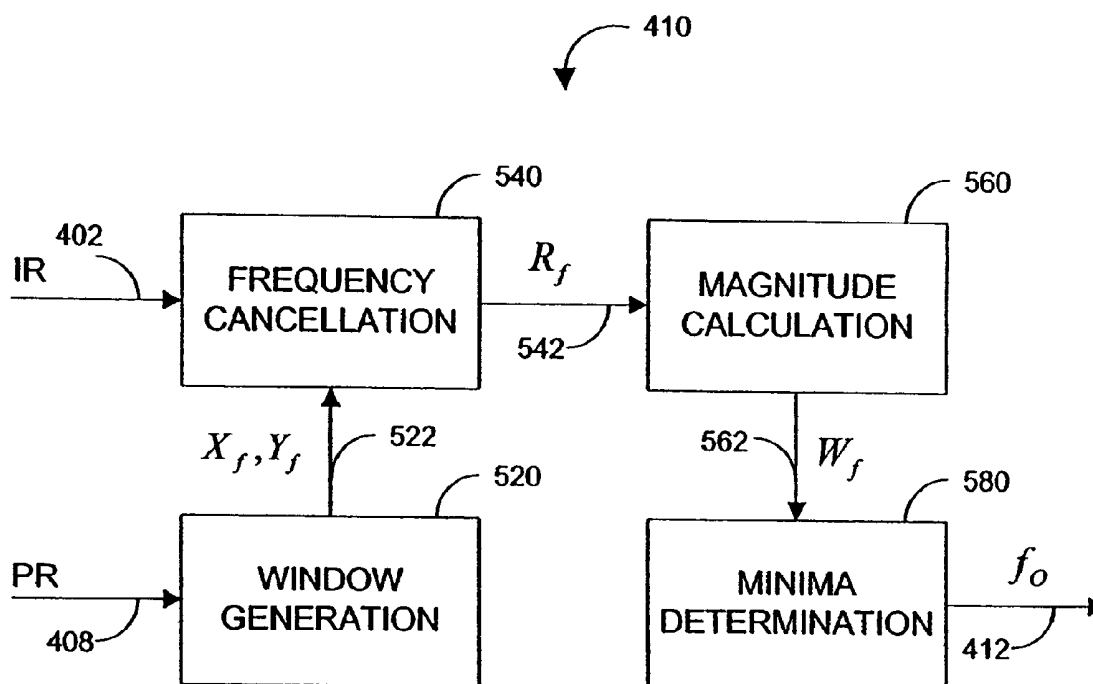
US 20090099429A1

(19) **United States**(12) **Patent Application Publication**  
**Weber et al.**(10) **Pub. No.: US 2009/0099429 A1**(43) **Pub. Date: Apr. 16, 2009**(54) **SINE SATURATION TRANSFORM**(76) Inventors: **Walter M. Weber**, Laguna Hills,  
CA (US); **Ammar Al-Ali**, Tustin,  
CA (US); **Lorenzo Cazzoli**,  
Barcelona (ES)

Correspondence Address:

**KNOBBE MARTENS OLSON & BEAR LLP**  
**2040 MAIN STREET, FOURTEENTH FLOOR**  
**IRVINE, CA 92614 (US)**(21) Appl. No.: **12/336,419**(22) Filed: **Dec. 16, 2008****Related U.S. Application Data**(63) Continuation of application No. 11/894,648, filed on  
Aug. 20, 2007, now Pat. No. 7,467,002, which is a  
continuation of application No. 11/417,914, filed on  
May 3, 2006, now Pat. No. 7,377,899, which is a  
continuation of application No. 11/048,232, filed onFeb. 1, 2005, now Pat. No. 7,373,194, which is a con-  
tinuation of application No. 10/184,032, filed on Jun.  
26, 2002, now Pat. No. 6,850,787.(60) Provisional application No. 60/302,438, filed on Jun.  
29, 2001.**Publication Classification**(51) **Int. Cl.**  
**A61B 5/1455** (2006.01)  
**G01R 29/00** (2006.01)(52) **U.S. Cl.** ..... **600/323; 600/324; 702/189**(57) **ABSTRACT**

A transform for determining a physiological measurement is disclosed. The transform determines a basis function index from a physiological signal obtained through a physiological sensor. A basis function waveform is generated based on basis function index. The basis function waveform is then used to determine an optimized basis function waveform. The optimized basis function waveform is used to calculate a physiological measurement.



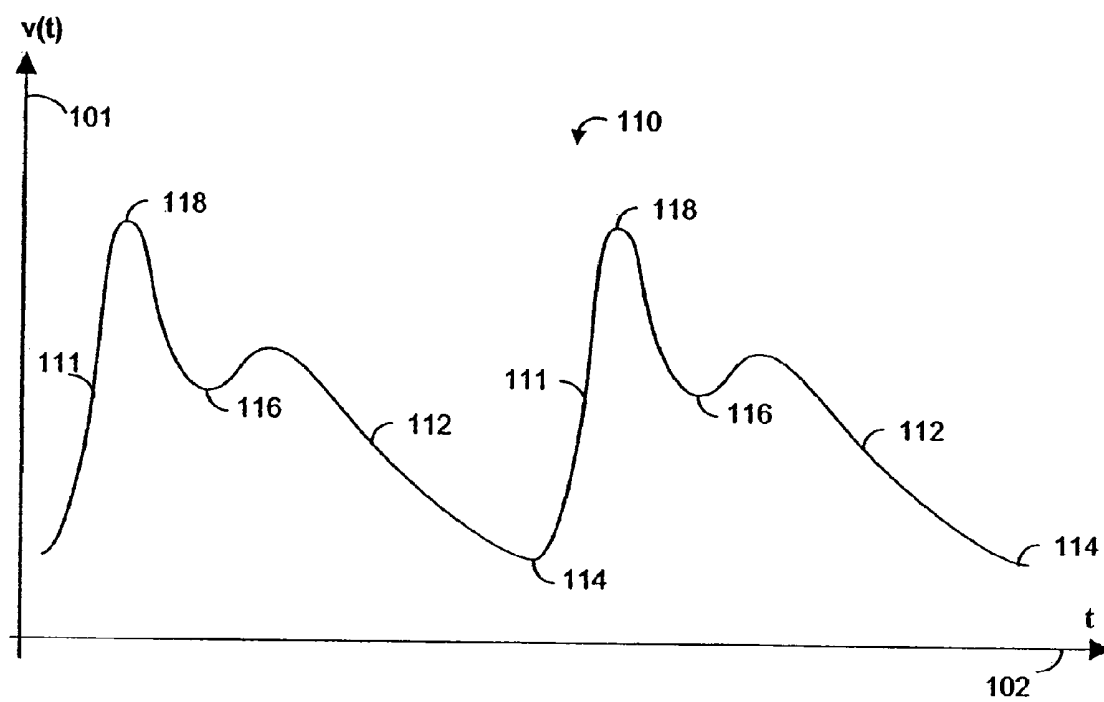


FIG. 1A

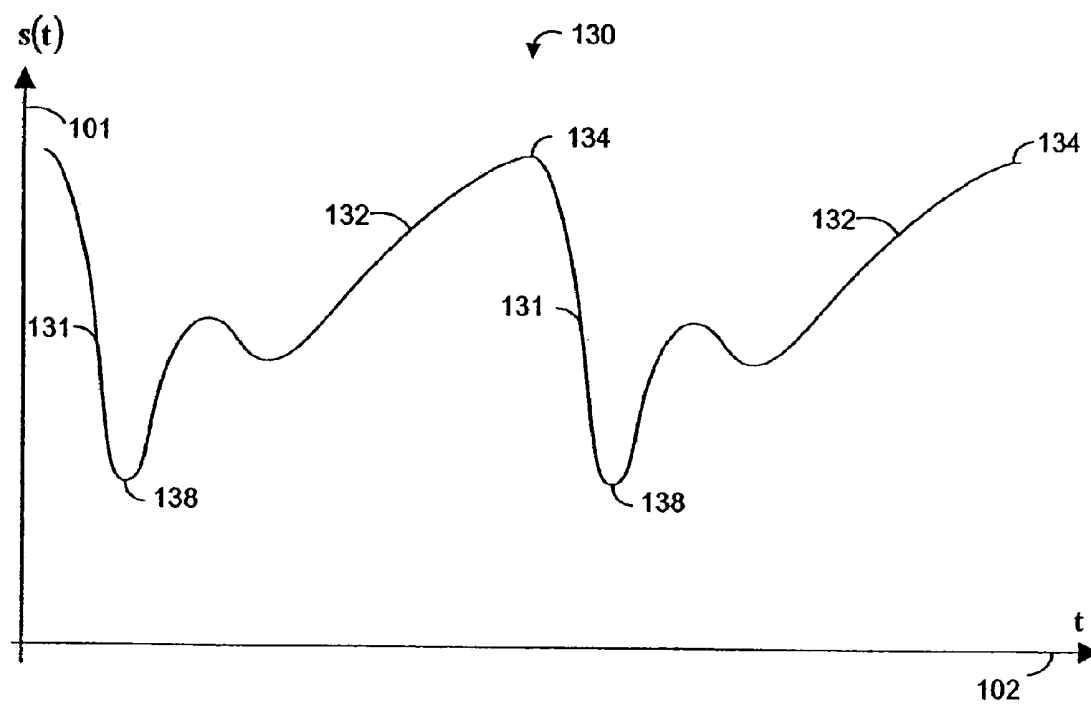


FIG. 1B

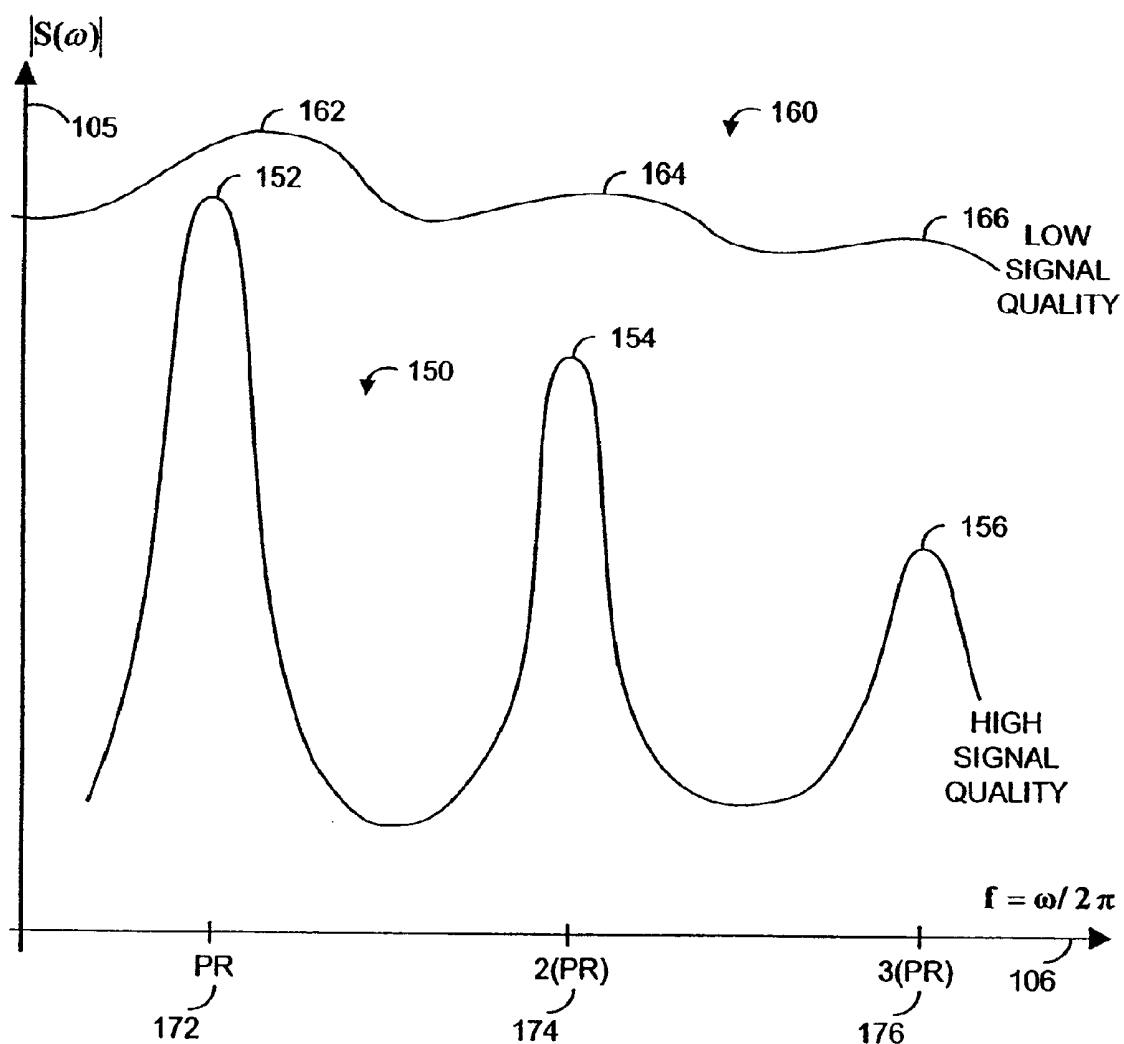


FIG. 1C

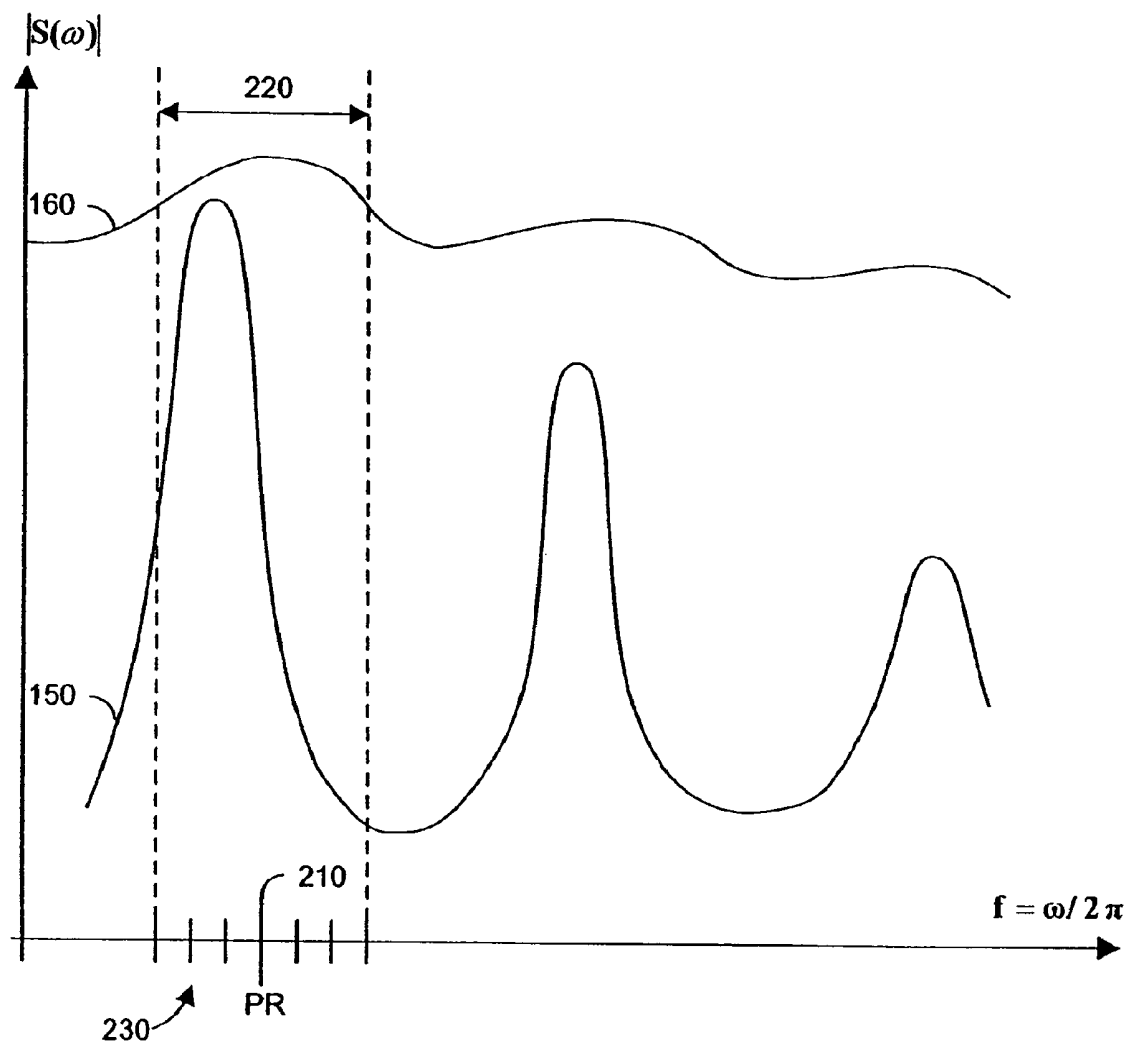


FIG. 2

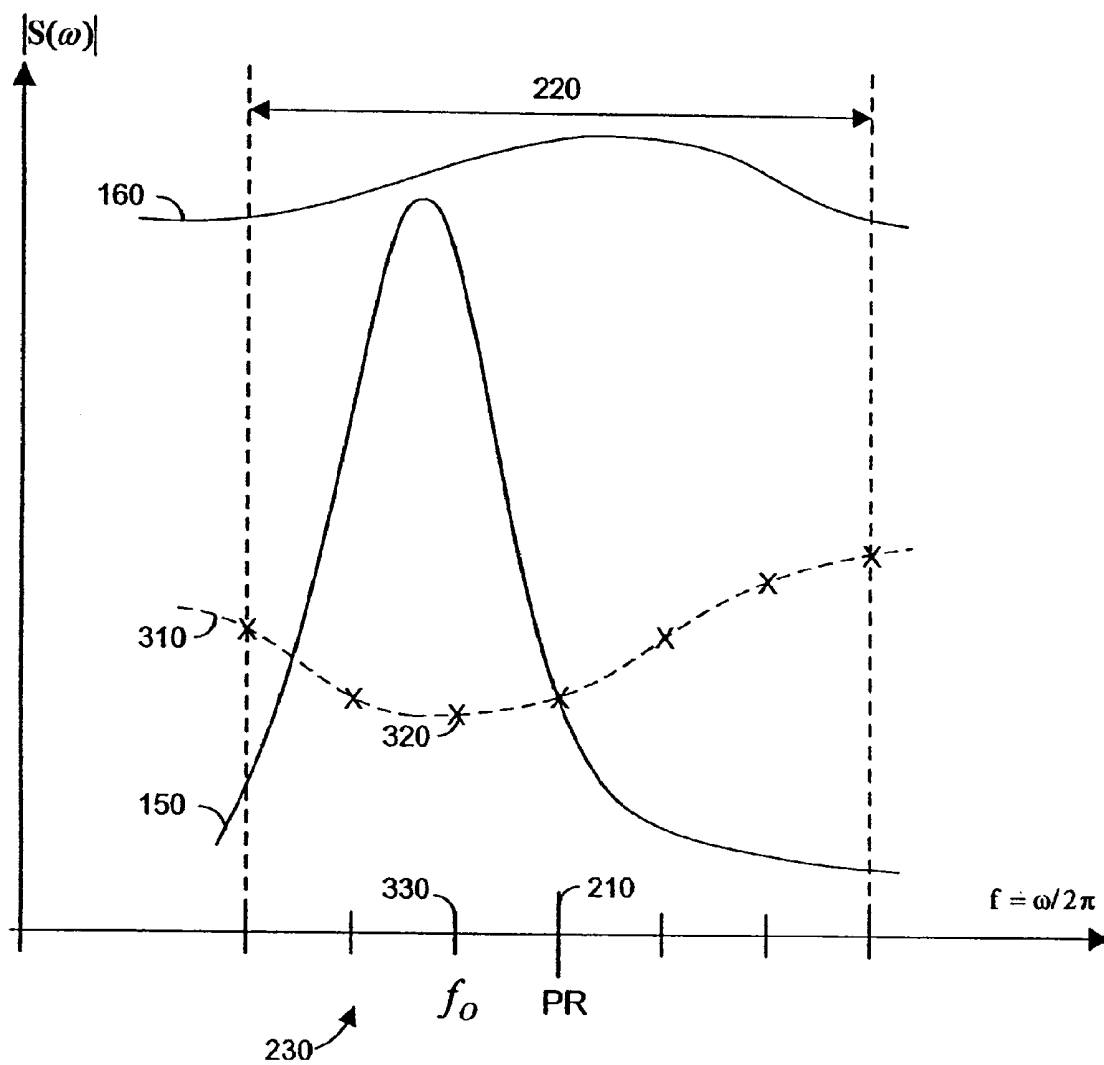
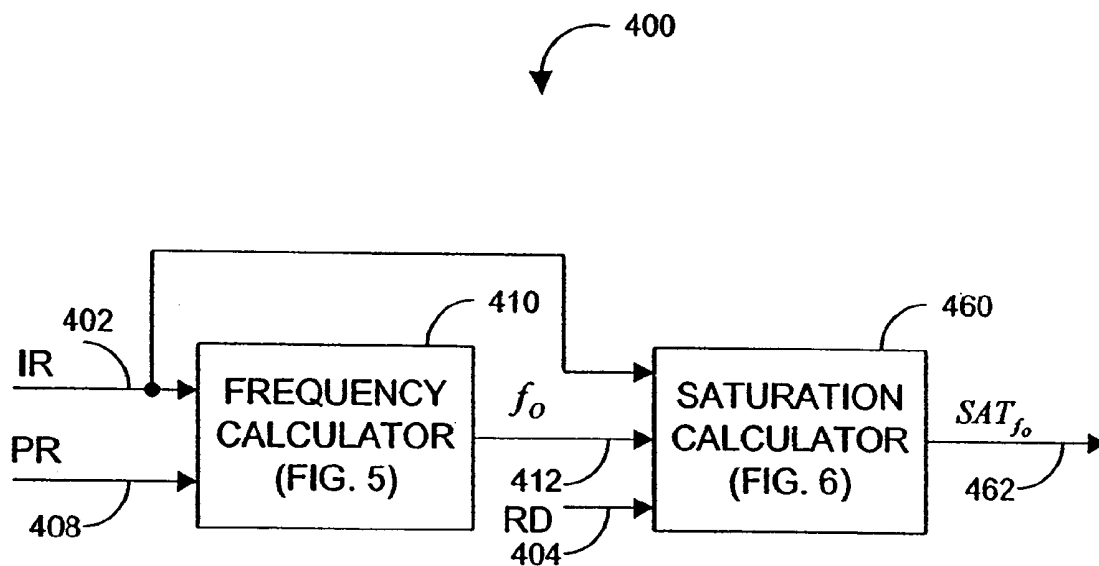


FIG. 3

**FIG. 4**

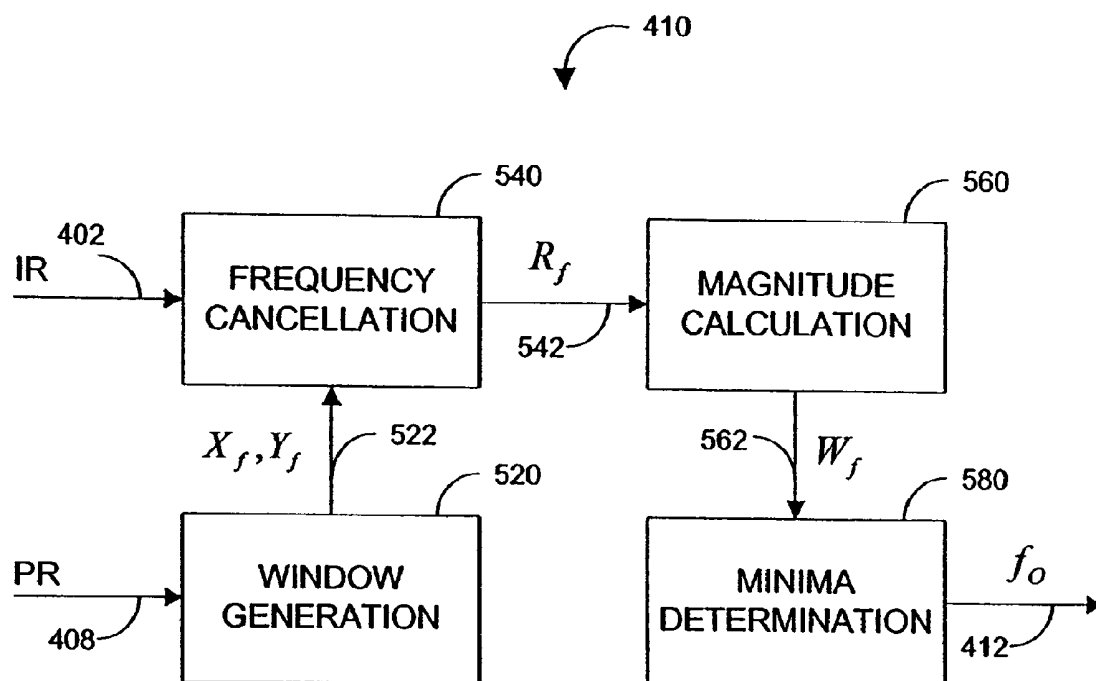


FIG. 5

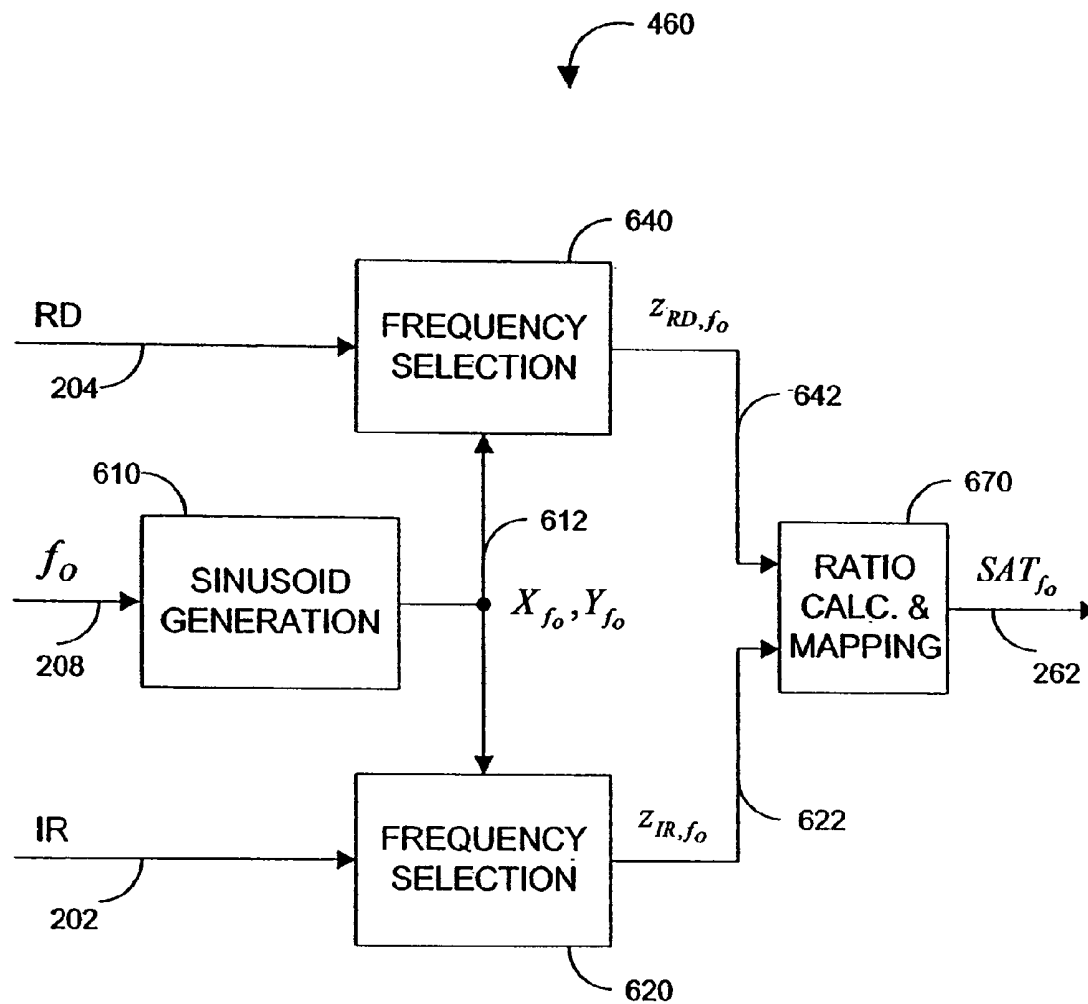


FIG. 6

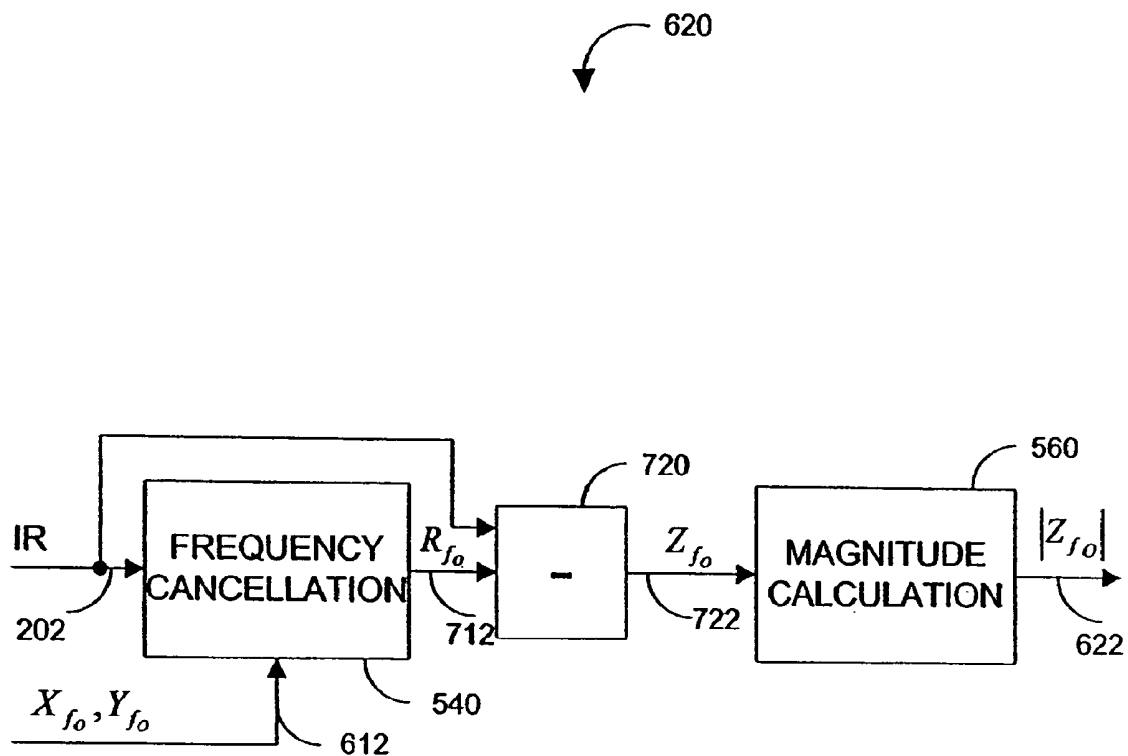


FIG. 7

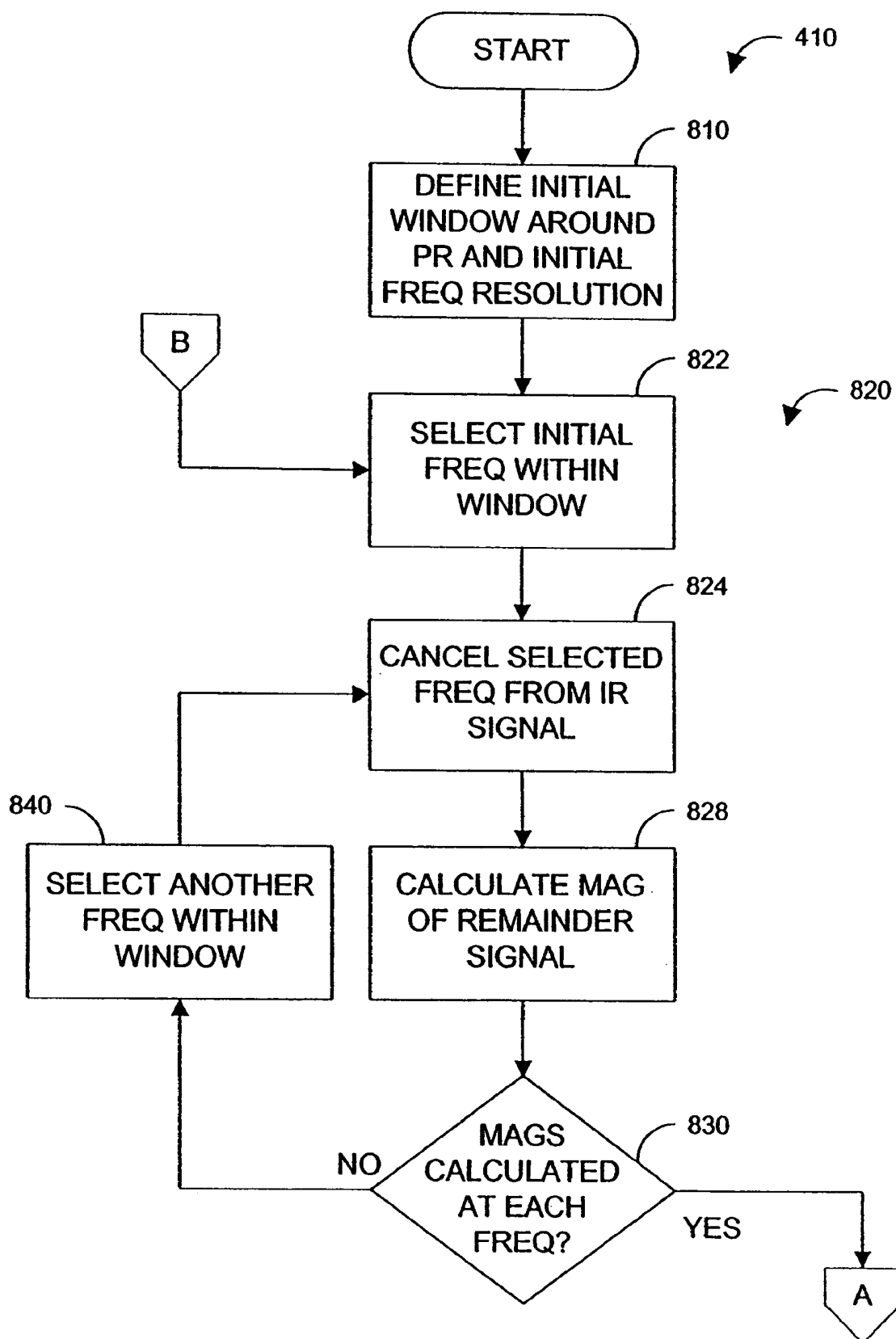


FIG. 8A

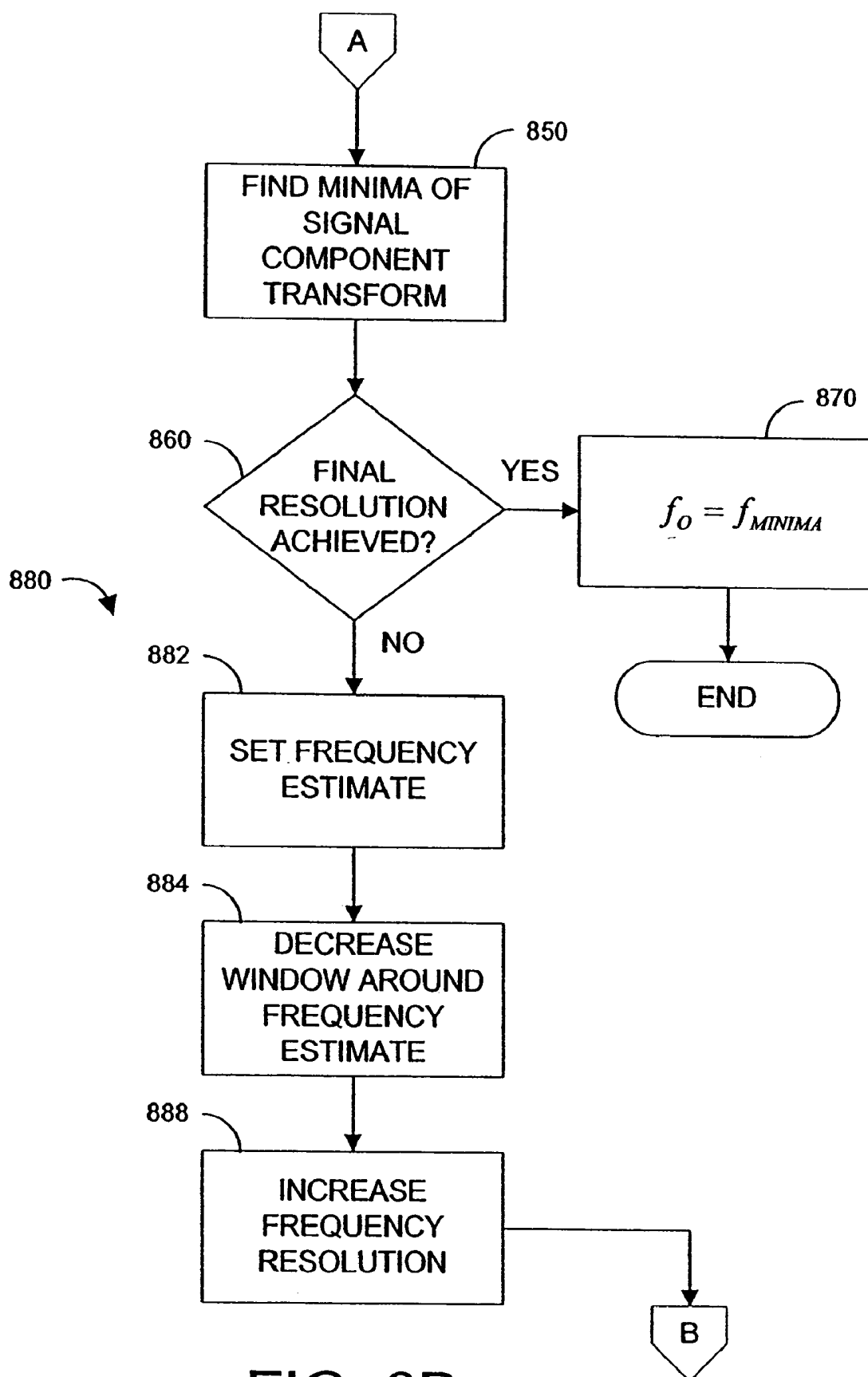


FIG. 8B

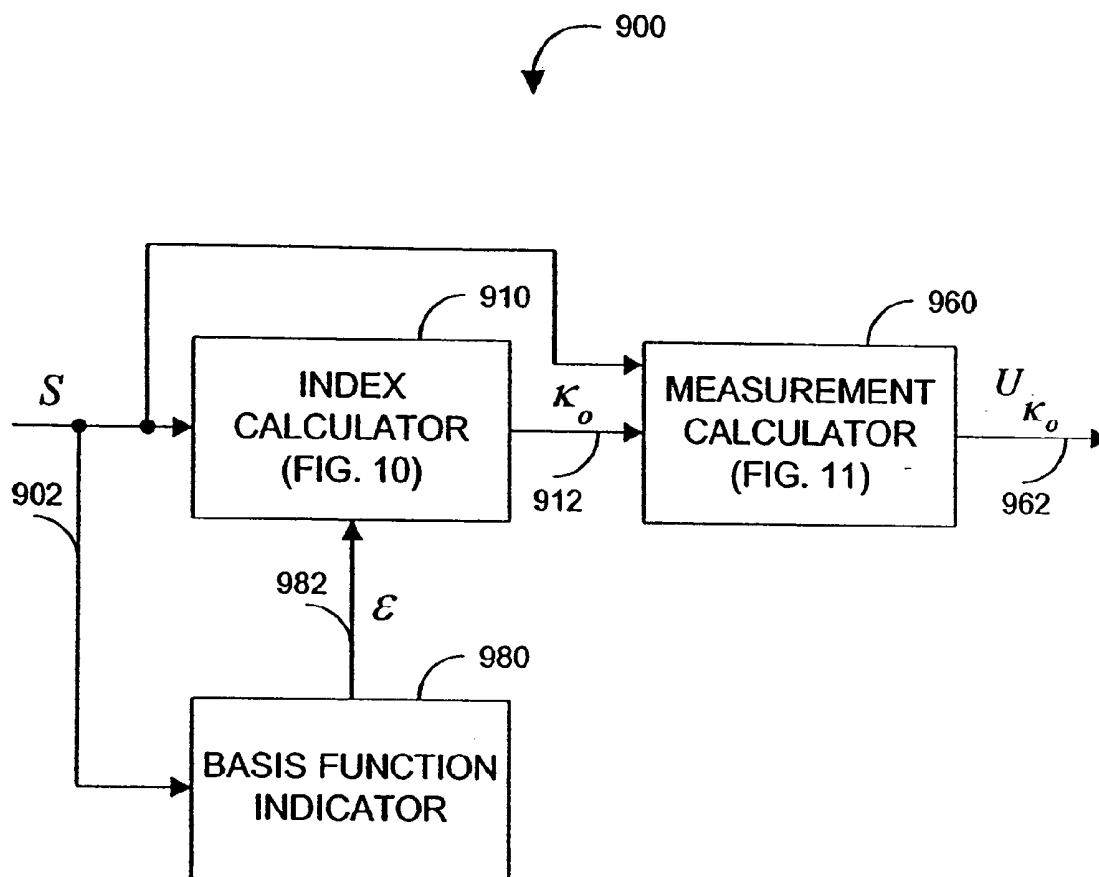


FIG. 9

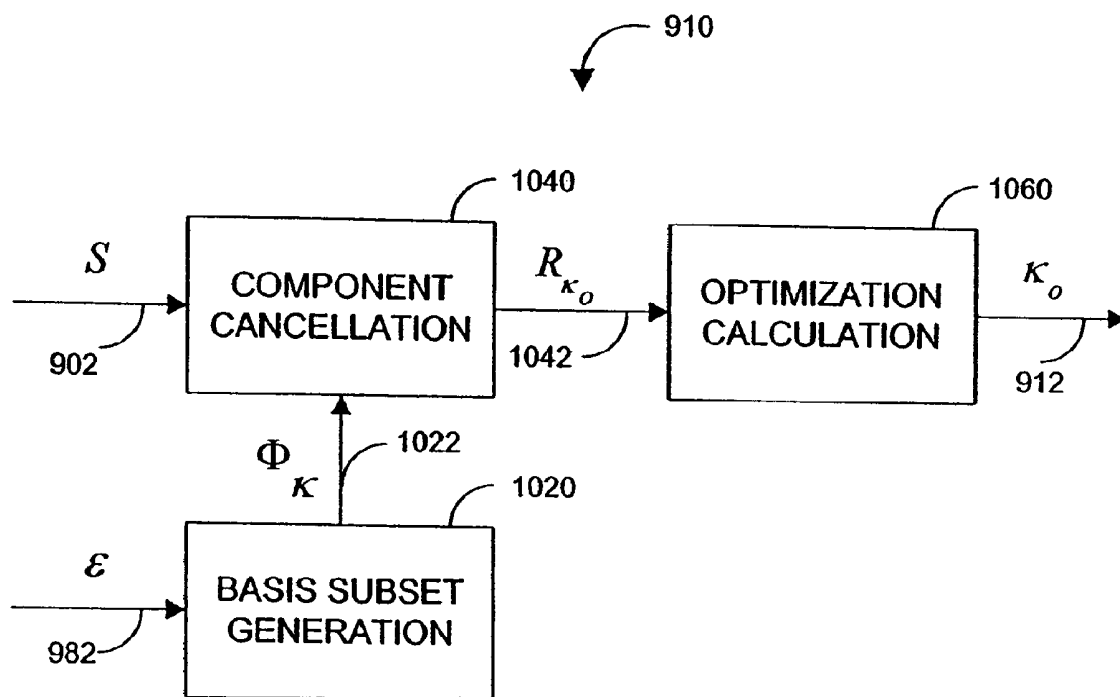


FIG. 10

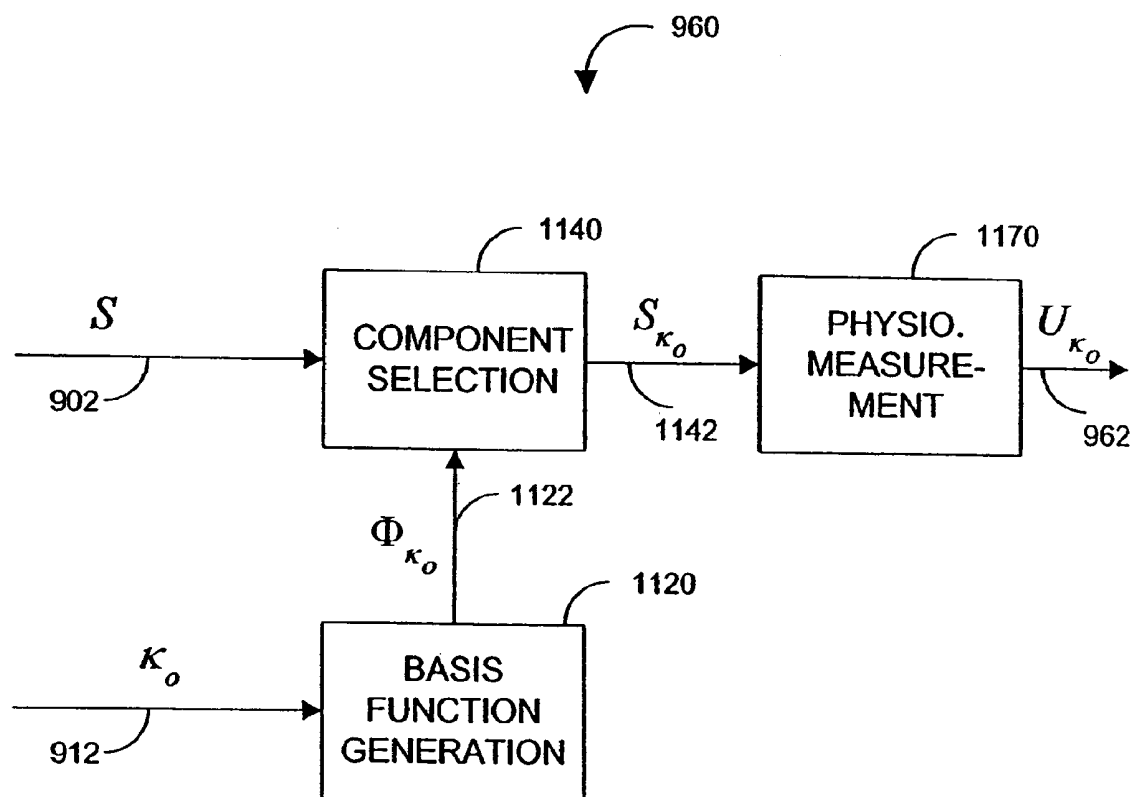


FIG. 11

## SINE SATURATION TRANSFORM

### CROSS-REFERENCE TO RELATED APPLICATIONS

[0001] The present application claims priority benefit under 35 U.S.C. § 120 to, and is a continuation of U.S. patent application Ser. No. 11/894,648, filed Aug. 20, 2007 entitled "Sine Saturation Transform," now U.S. Pat. No. 7,467,002 which is a continuation of U.S. patent application Ser. No. 11/417,914, filed May 3, 2006, entitled "Sine Saturation Transform," now U.S. Pat. No. 7,377,899, which is a continuation of, U.S. patent application Ser. No. 11/048,232, filed Feb. 1, 2005, entitled "Signal Component Processor," now U.S. Pat. No. 7,373,194 which is a continuation of U.S. patent application Ser. No. 10/184,032, filed Jun. 26, 2002, entitled "Signal Component Processor," now U.S. Pat. No. 6,850,787, which claims priority benefit under 35 U.S.C. § 119(e) from U.S. Provisional Application No. 60/302,438, filed Jun. 29, 2001, entitled "Signal Component Processor." The present application also incorporates the foregoing disclosures herein by reference.

### BACKGROUND OF THE INVENTION

[0002] Early detection of low blood oxygen is critical in the medical field, for example in critical care and surgical applications, because an insufficient supply of oxygen can result in brain damage and death in a matter of minutes. Pulse oximetry is a widely accepted noninvasive procedure for measuring the oxygen saturation level of arterial blood, an indicator of oxygen supply. A pulse oximeter typically provides a numerical readout of the patient's oxygen saturation and pulse rate. A pulse oximetry system consists of a sensor attached to a patient, a monitor, and a cable connecting the sensor and monitor. Conventionally, a pulse oximetry sensor has both red (RD) and infrared (IR) light-emitting diode (LED) emitters and a photodiode detector. The pulse oximeter measurements are based upon the absorption by arterial blood of the two wavelengths emitted by the sensor. The pulse oximeter alternately activates the RD and IR sensor emitters and reads the resulting RD and IR sensor signals, i.e. the current generated by the photodiode in proportion to the detected RD and IR light intensity, in order to derive an arterial oxygen saturation value, as is well-known in the art. A pulse oximeter contains circuitry for controlling the sensor, processing the sensor signals and displaying the patient's oxygen saturation and pulse rate.

### SUMMARY OF THE INVENTION

[0003] FIG. 1A illustrates a plethysmograph waveform 110, which is a display of blood volume, shown along the ordinate 101, over time, shown along the abscissa 102. The shape of the plethysmograph waveform 110 is a function of heart stroke volume, pressure gradient, arterial elasticity and peripheral resistance. Ideally, the waveform 110 displays a short, steep inflow phase 111 during ventricular systole followed by a typically three to four times longer outflow phase 112 during diastole. A dicrotic notch 116 is generally attributed to closure of the aortic valve at the end of ventricular systole.

[0004] FIG. 1B illustrates a corresponding RD or IR sensor signal  $s(t)$  130, such as described above. The typical plethysmograph waveform 110 (FIG. 1A), being a function of blood volume, also provides a light absorption profile. A pulse

oximeter, however, does not directly detect light absorption and, hence, does not directly measure the plethysmograph waveform 110. However, IR or RD sensor signals are 180° out-of-phase versions of the waveform 110. That is, peak detected intensity 134 occurs at minimum absorption 114 and minimum detected intensity 138 occurs at maximum absorption 118.

[0005] FIG. 1C illustrates the corresponding spectrum of  $s(t)$ , which is a display of signal spectral magnitude  $|S(\omega)|$ , shown along the ordinate 105, versus frequency, shown along the abscissa 106. The plethysmograph spectrum is depicted under both high signal quality 150 and low signal quality 160 conditions. Low signal quality can result when a pulse oximeter sensor signal is distorted by motion-artifact and noise. Signal processing technologies such as described in U.S. Pat. No. 5,632,272, assigned to the assignee of the present invention and incorporated by reference herein, allow pulse oximetry to function through patient motion and other low signal quality conditions.

[0006] Ideally, plethysmograph energy is concentrated at the pulse rate frequency 172 and associated harmonics 174, 176. Accordingly, motion-artifact and noise may be reduced and pulse oximetry measurements improved by filtering out sensor signal frequencies that are not related to the pulse rate. Under low signal quality conditions, however, the frequency spectrum is corrupted and the pulse rate fundamental 152 and harmonics 154, 156 can be obscured or masked, resulting in errors in the computed pulse rate. In addition, a pulse rate, physiologically, is dynamic, potentially varying significantly between different measurement periods. Hence, maximum plethysmograph energy may not correspond to the computed pulse rate except under high signal quality conditions and stable pulse rates. Further, an oxygen saturation value calculated from an optical density ratio, such as a normalized red over infrared ratio, at the pulse rate frequency can be sensitive to computed pulse rate errors. In order to increase the robustness of oxygen saturation measurements, therefore, it is desirable to improve pulse rate based measurements by identifying sensor signal components that correspond to an optimization, such as maximum signal energy.

[0007] One aspect of a signal component processor comprises a physiological signal, a basis function index determined from the signal, a basis function waveform generated according to the index, a component derived from the sensor signal and the waveform, and a physiological measurement responsive to the component. In one embodiment, the component is responsive to the inner product of the sensor signal and the waveform. In another embodiment, the index is a frequency and the waveform is a sinusoid at the frequency. In that embodiment, the signal processor may further comprise a pulse rate estimate derived from the signal wherein the frequency is selected from a window including the pulse rate estimate. The physiological measurement may be an oxygen saturation value responsive to a magnitude of the component.

[0008] Another aspect of a signal component processor comprises a signal input, a basis function indicator derived from the signal input, a plurality of basis functions generated according to the indicator, a plurality of characteristics of the signal input corresponding to the basis functions and an optimization of the characteristics so as to identify at least one of said basis functions. In one embodiment, the indicator is a pulse rate estimate and the processor further comprises a window configured to include the pulse rate estimate, and a plurality of frequencies selected from within the window. In

another embodiment, the characteristic comprises a plurality of signal remainders corresponding to the basis functions and a plurality of magnitudes of the signal remainders. In that embodiment, the optimization comprises a minima of the magnitudes. In a further embodiment, the characteristic comprises a plurality of components corresponding to the basis functions and a plurality of magnitudes of the components. In this embodiment, the optimization comprises a maxima of the magnitudes.

**[0009]** An aspect of a signal component processing method comprises the steps of receiving a sensor signal, calculating an estimated pulse rate, determining an optimization of the sensor signal proximate the estimated pulse rate, defining a frequency corresponding to the optimization, and outputting a physiological measurement responsive to a component of the sensor signal at the frequency. In one embodiment the determining step comprises the substeps of transforming the sensor signal to a frequency spectrum encompassing the estimated pulse rate and detecting an extrema of the spectrum indicative of the frequency. The transforming step may comprise the substeps of defining a window including the estimated pulse rate, defining a plurality of selected frequencies within the window, canceling the selected frequencies, individually, from the sensor signal to generate a plurality of remainder signals and calculating a plurality of magnitudes of the remainder signals. The detecting step may comprise the substep of locating a minima of the magnitudes.

**[0010]** In another embodiment, the outputting step comprises the substeps of inputting a red (RD) portion and an infrared (IR) portion of the sensor signal, deriving a RD component of the RD portion and an IR component of the IR portion corresponding to the frequency and computing an oxygen saturation based upon a magnitude ratio of the RD component and the IR component. The deriving step may comprise the substeps of generating a sinusoidal waveform at the frequency and selecting the RD component and the IR component utilizing the waveform. The selecting step may comprise the substep of calculating the inner product between the waveform and the RD portion and the inner product between the waveform and the IR portion. The selecting step may comprise the substeps of canceling the waveform from the RD portion and the IR portion, leaving a RD remainder and an IR remainder, and subtracting the RD remainder from the RD portion and the IR remainder from the IR portion.

**[0011]** A further aspect of a signal component processor comprises a first calculator means for deriving an optimization frequency from a pulse rate estimate input and a sensor signal, and a second calculator means for deriving a physiological measurement responsive to a sensor signal component at the frequency. In one embodiment, the first calculator means comprises a signal component transform means for determining a plurality of signal values corresponding to a plurality of selected frequencies within a window including the pulse rate estimate, and a detection means for determining a particular one of the selected frequencies corresponding to an optimization of the sensor signal. The second calculator means may comprise a waveform means for generating a sinusoidal signal at the frequency, a frequency selection means for determining a component of the sensor signal from the sinusoidal signal and a calculator means for deriving a ratio responsive to the component.

#### BRIEF DESCRIPTION OF THE DRAWINGS

**[0012]** FIGS. 1A-C are graphical representations of a pulse oximetry sensor signal;

**[0013]** FIG. 1A is a typical plethysmograph illustrating blood volume versus time;

**[0014]** FIG. 1B is a pulse oximetry sensor signal illustrating detected light intensity versus time;

**[0015]** FIG. 1C is a pulse oximetry sensor signal spectrum illustrating both high signal quality and low signal quality conditions;

**[0016]** FIGS. 2-3 are magnitude versus frequency graphs for a pulse oximetry sensor signal illustrating an example of signal component processing;

**[0017]** FIG. 2 illustrates a frequency window around an estimated pulse rate; and

**[0018]** FIG. 3 illustrates an associated signal component transform;

**[0019]** FIGS. 4-7 are functional block diagrams of one embodiment of a signal component processor;

**[0020]** FIG. 4 is a top-level functional block diagram of a signal component processor;

**[0021]** FIG. 5 is a functional block diagram of a frequency calculator;

**[0022]** FIG. 6 is a functional block diagram of a saturation calculator; and

**[0023]** FIG. 7 is a functional block diagram of one embodiment of a frequency selection;

**[0024]** FIGS. 8A-B are flowcharts of an iterative embodiment of a frequency calculator; and

**[0025]** FIGS. 9-11 are functional block diagrams of another embodiment of a signal component processor;

**[0026]** FIG. 9 is a top-level functional block diagram of a signal component processor;

**[0027]** FIG. 10 is a functional block diagram of an index calculator; and

**[0028]** FIG. 11 is a functional block diagram of a measurement calculator.

#### DETAILED DESCRIPTION OF THE PREFERRED EMBODIMENTS

**[0029]** FIGS. 2 and 3 provide graphical illustration examples of signal component processing. Advantageously, signal component processing provides a direct method for the calculation of saturation based on pulse rate. For example, it is not necessary to compute a frequency transform, such as an FFT, which derives an entire frequency spectrum. Rather, signal component processing singles out specific signal components, as described in more detail below. Further, signal component processing advantageously provides a method of refinement for the calculation of saturation based on pulse rate.

**[0030]** FIG. 2 illustrates high and low signal quality sensor signal spectrums **150**, **160** as described with respect to FIG. 1C, above. A frequency window **220** is created, including a pulse rate estimate **PR 210**. A pulse rate estimate can be calculated as disclosed in U.S. Pat. No. 6,002,952, entitled "Signal Processing Apparatus and Method," assigned to the assignee of the present invention and incorporated by reference herein. A search is conducted within this window **220** for a component frequency  $f_o$  at an optimization. In particular, selected frequencies **230**, which include **PR**, are defined within the window **220**. The components of a signals(t) at each of these frequencies **230** are then examined for an optimization indicative of an extrema of energy, power or other signal characteristic. In an alternative embodiment, the com-

ponents of the signals(t) are examined for an optimization over a continuous range of frequencies within the window 220.

[0031] FIG. 3 illustrates an expanded portion of the graph described with respect to FIG. 2, above. Superimposed on the high signal quality 150 and low signal quality 160 spectrums is a signal component transform 310. In one embodiment, a signal component transform 310 is indicative of sensor signal energy and is calculated at selected signal frequencies 230 within the window 220. A signal component transform 310 has an extrema 320 that indicates, in this embodiment, energy optimization at a particular one 330 of the selected frequencies 230. The extrema 320 can be, for example, a maxima, minima or inflection point. In the embodiment illustrated, each point of the transform 310 is the magnitude of the signal remaining after canceling a sensor signal component at one of the selected frequencies. The extrema 320 is a minima, which indicates that canceling the corresponding frequency 330 removes the most signal energy. In an alternative embodiment, not illustrated, the transform 310 is calculated as the magnitude of signal components at each of the selected frequencies 230. In that embodiment, the extrema is a maxima, which indicates the largest energy signal at the corresponding frequency. The result of a signal component transform 310 is identification of a frequency  $f_o$  330 determined from the frequency of a signal component transform extrema 320. Frequency  $f_o$  330 is then used to calculate an oxygen saturation. A signal component transform and corresponding oxygen saturation calculations are described in additional detail with respect to FIGS. 4-8, below. Although signal component processing is described above with respect to identifying a particular frequency within a window including a pulse rate estimate PR, a similar procedure could be performed on 2PR, 3PR etc. resulting in the identification of multiple frequencies  $f_{o1}$ ,  $f_{o2}$ , etc., which could be used for the calculation of oxygen saturation as well.

[0032] Advantageously, a signal component transform 310 is calculated over any set of selected frequencies, unrestricted by the number or spacing of these frequencies. In this manner, a signal component transform 310 differs from a FFT or other standard frequency transforms. For example, a FFT is limited to N evenly-distributed frequencies spaced at a resolution of  $f_s/N$ , where N is the number of signal samples and  $f_s$  is the sampling frequency. That is, for a FFT, a relatively high sampling rate or a relatively large record length or both are needed to achieve a relatively high resolution in frequency. Signal component processing, as described herein, is not so limited. Further, a signal component transform 310 is advantageously calculated only over a range of frequencies of interest. A FFT or similar frequency transformation may be computationally more burdensome than signal component processing, in part because such a transform is computed over all frequencies within a range determined by the sampling frequency,  $f_s$ .

[0033] FIGS. 4-7 illustrate one embodiment of a signal component processor. FIG. 4 is a top-level functional block diagram of a signal component processor 400. The signal component processor 400 has a frequency calculator 410 and a saturation calculator 460. The frequency calculator 410 has an IR signal input 402, a pulse rate estimate signal PR input 408 and a component frequency  $f_o$  output 412. The frequency calculator 410 performs a signal component transform based upon the PR input 408 and determines the  $f_o$  output 412, as

described with respect to FIGS. 2-3, above. The frequency calculator 410 is described in further detail with respect to FIG. 5, below.

[0034] In an alternative embodiment, the frequency calculator 410 determines  $f_o$  412 based upon a RD signal input substituted for, or in addition to, the IR signal input 402. Similarly, one of ordinary skill in the art will recognize that  $f_o$  can be determined by the frequency calculator 410 based upon one or more inputs responsive to a variety of sensor wavelengths.

[0035] The saturation calculator 460 has an IR signal input 402, a RD signal input 404, a component frequency  $f_o$  input 412 and an oxygen saturation output, SAT $_{f_o}$  462. The saturation calculator 460 determines values of the IR signal input 402 and the RD signal input 404 at the component frequency  $f_o$  412 and computes a ratio of those values to determine SAT $_{f_o}$  462, as described with respect to FIG. 6, below. The IR signal input 402 and RD signal input 404 can be expressed as:

$$IR = \begin{bmatrix} IR_0 \\ \vdots \\ IR_{N-1} \end{bmatrix}; RD = \begin{bmatrix} RD_0 \\ \vdots \\ RD_{N-1} \end{bmatrix} \quad (1)$$

[0036] where N is the number of samples of each signal input.

[0037] FIG. 5 shows one embodiment of the frequency calculator 410. In this particular embodiment, the frequency calculator functions are window generation 520, frequency cancellation 540, magnitude calculation 560 and minima determination 580. Window generation 520, frequency cancellation 540 and magnitude calculation 560 combine to create a signal component transform 310 (FIG. 3), as described with respect to FIG. 3, above. Minima determination 580 locates the signal component transform extrema 320 (FIG. 3), which identifies  $f_o$  412, also described with respect to FIG. 3, above.

[0038] As shown in FIG. 5, window generation 520 has a PR input 408 and defines a window 220 (FIG. 3) about PR 210 (FIG. 3) including a set of selected frequencies 230 (FIG. 3)

$$\{f_m; m = 0, \dots, M-1\}; f = \begin{bmatrix} f_0 \\ \vdots \\ f_{M-1} \end{bmatrix} \quad (2)$$

[0039] where M is the number of selected frequencies 230 (FIG. 3) within the window 220 (FIG. 3). Window generation 520 has a sinusoidal output  $X_f$ ,  $Y_f$  522, which is a set of sinusoidal waveforms  $x_{n,f}$ ,  $y_{n,f}$  each corresponding to one of the set of selected frequencies 230 (FIG. 3). Specifically

$$X_f = \begin{bmatrix} x_{0,f} \\ \vdots \\ x_{N-1,f} \end{bmatrix}; Y_f = \begin{bmatrix} y_{0,f} \\ \vdots \\ y_{N-1,f} \end{bmatrix} \quad (3a)$$

$$x_{n,f} = \sin(2\pi f n); y_{n,f} = \cos(2\pi f n) \quad (4b)$$

[0040] Also shown in FIG. 5, the frequency cancellation 540 has IR 402 and  $X_f$ ,  $Y_f$  522 inputs and a remainder output  $R_f$  542, which is a set of remainder signals  $r_{n,f}$  each corre-

sponding to one of the sinusoidal waveforms  $x_{n,f}$ ,  $y_{n,f}$ . For each selected frequency  $f$  **230** (FIG. 3), frequency cancellation **540** cancels that frequency component from the input signal **IR 402** to generate a remainder signal  $r_{n,f}$ . In particular, frequency cancellation **540** generates a remainder  $R_f$  **542**

$$R_f = \begin{bmatrix} r_{0,f} \\ \vdots \\ r_{N-1,f} \end{bmatrix} \quad (4a)$$

$$R_f = IR - \frac{IR \cdot X_f}{|X_f|^2} X_f - \frac{IR \cdot Y_f}{|Y_f|^2} Y_f \quad (4b)$$

**[0041]** Additionally, as shown in FIG. 5, the magnitude calculation **560** has a remainder input  $R_f$  **542** and generates a magnitude output  $W_f$  **562**, where

$$W_f = |R_f| = \sqrt{\sum_{n=0}^{N-1} r_{n,f}^2} \quad (5)$$

**[0042]** Further shown in FIG. 5, the minima determination **580** has the magnitude values  $W_f$  **562** as inputs and generates a component frequency  $f_o$  output. Frequency  $f_o$  is the particular frequency associated with the minimum magnitude value

$$W_{f_o} = \min\{W_f\} \quad (6)$$

**[0043]** FIG. 6 shows that the saturation calculator **460** functions are sinusoid generation **610**, frequency selection **620**, **640** and ratio calculation **670**. Sinusoid generation has a component frequency  $f_o$  input **208** and a sinusoidal waveform  $X_{f_o}$ ,  $Y_{f_o}$  output **612**, which has a frequency of  $f_o$ . Frequency selection **620**, **640** has a sensor signal input, which is either an IR signal **202** or a RD signal **204** and a sinusoid waveform  $X_{f_o}$ ,  $Y_{f_o}$  input **612**. Frequency selection **620**, **640** provides magnitude outputs  $Z_{IR,f_o}$  **622** and  $Z_{RD,f_o}$  **642** which are the frequency components of the IR **202** and RD **204** sensor signals at the  $f_o$  frequency. Specifically, from equation 3(a)

$$X_{f_o} = \begin{bmatrix} x_{0,f_o} \\ \vdots \\ x_{N-1,f_o} \end{bmatrix}; Y_{f_o} = \begin{bmatrix} y_{0,f_o} \\ \vdots \\ y_{N-1,f_o} \end{bmatrix} \quad (7)$$

**[0044]** Then, referring to equation 1

$$z_{IR,f_o} = \left| \frac{IR \cdot X_{f_o}}{|X_{f_o}|^2} X_{f_o} + \frac{IR \cdot Y_{f_o}}{|Y_{f_o}|^2} Y_{f_o} \right| \quad (8a)$$

$$= \sqrt{\frac{(IR \cdot X_{f_o})^2}{|X_{f_o}|^2} + \frac{(IR \cdot Y_{f_o})^2}{|Y_{f_o}|^2}}$$

$$z_{RD,f_o} = \left| \frac{RD \cdot X_{f_o}}{|X_{f_o}|^2} X_{f_o} + \frac{RD \cdot Y_{f_o}}{|Y_{f_o}|^2} Y_{f_o} \right| \quad (8b)$$

$$= \sqrt{\frac{(RD \cdot X_{f_o})^2}{|X_{f_o}|^2} + \frac{(RD \cdot Y_{f_o})^2}{|Y_{f_o}|^2}}$$

**[0045]** For simplicity of illustration, EQS. 8a-b assume that the cross-product of  $X_{f_o}$  and  $Y_{f_o}$  is zero, although generally this is not the case. The ratio calculation and mapping **670** has  $Z_{IR,f_o}$  **622** and  $Z_{RD,f_o}$  **642** as inputs and provides  $SAT_{f_o}$  **262** as an output. That is

$$SAT_{f_o} = g\{Z_{RD,f_o}/Z_{IR,f_o}\} \quad (9)$$

**[0046]** where  $g$  is a mapping of the red-over-IR ratio to oxygen saturation, which may be an empirically derived lookup table, for example.

**[0047]** FIG. 7 illustrates an alternative embodiment of frequency selection **620** (FIG. 6), as described above. In this embodiment, frequency cancellation **540** and magnitude calculation **560**, as described with respect to FIG. 5, can also be used, advantageously, to perform frequency selection. Specifically, frequency cancellation **540** has IR **202** and  $X_{f_o}$ ,  $Y_{f_o}$  **612** as inputs and generates a remainder signal  $R_{f_o}$  **712** as an output, where

$$R_{f_o} = IR - \frac{IR \cdot X_{f_o}}{|X_{f_o}|^2} X_{f_o} - \frac{IR \cdot Y_{f_o}}{|Y_{f_o}|^2} Y_{f_o} \quad (10)$$

**[0048]** The remainder  $R_{f_o}$  **712** is subtracted **720** from IR **202** to yield

$$\begin{aligned} Z_{f_o} &= IR - \left[ IR - \frac{IR \cdot X_{f_o}}{|X_{f_o}|^2} X_{f_o} - \frac{IR \cdot Y_{f_o}}{|Y_{f_o}|^2} Y_{f_o} \right] \\ &= \frac{IR \cdot X_{f_o}}{|X_{f_o}|^2} X_{f_o} + \frac{IR \cdot Y_{f_o}}{|Y_{f_o}|^2} Y_{f_o} \end{aligned} \quad (11)$$

**[0049]** where  $z_{f_o}$  **722** is the component of IR **202** at the  $f_o$  frequency. The magnitude calculation **560** has  $z_{f_o}$  **722** as an input and calculates

$$\begin{aligned} |Z_{f_o}| &= \left| \frac{IR \cdot X_{f_o}}{|X_{f_o}|^2} X_{f_o} + \frac{IR \cdot Y_{f_o}}{|Y_{f_o}|^2} Y_{f_o} \right| \\ &= \sqrt{\frac{(IR \cdot X_{f_o})^2}{|X_{f_o}|^2} + \frac{(IR \cdot Y_{f_o})^2}{|Y_{f_o}|^2}} \end{aligned} \quad (12)$$

**[0050]** which is equivalent to equation 8a, above.

**[0051]** FIGS. 8A-B illustrate an iterative embodiment of the frequency calculator **410** (FIG. 4) described above. An iterative frequency calculator **410** has an initialization **810**, a signal component transform **820**, an extrema detection **850**, a resolution decision **860** and a resolution refinement **880** and provides a component frequency  $f_o$  **870**. Initialization **810** defines a window around the pulse rate estimate PR and a frequency resolution within that window.

**[0052]** As shown in FIG. 8A, a signal component transform **820** has an initial frequency selection **822**, a frequency cancellation **824** and an magnitude calculation **828**. A decision block **830** determines if the magnitude calculation **828** has been performed at each frequency within the window. If not, the loop of frequency cancellation **824** and magnitude calculation **828** is repeated for another selected frequency in the window. The frequency cancellation **824** removes a frequency component from the IR sensor signal, as described with respect to FIG. 5, above. The magnitude calculation **828**

determines the magnitude of the remainder signal, also described with respect to FIG. 5, above. If the decision block 830 determines that the remainder signal magnitudes have been calculated at each of the selected frequencies, then the signal component transform loop 820 is exited to the steps described with respect to FIG. 8B.

[0053] As shown in FIG. 8B, the extrema detector 850 finds a minima of a signal component transform 820 and a resolution decision block 860 determines if the final frequency resolution of a signal component transform is achieved. If not, resolution refinement 880 is performed. If the final resolution is achieved, the component frequency output  $f_o$  is equated to the frequency of the minima 870, i.e. a signal component transform minima determined by the extrema detector 850.

[0054] Further shown in FIG. 8B, the resolution refinement 880 has a set frequency estimate 882, a window decrease 884 and a frequency resolution increase 888. Specifically, the frequency estimate 882 is set to a signal component transform minima, as determined by the extrema detector 850. The window decrease 884 defines a new and narrower window around the frequency estimate, and the frequency resolution increase 888 reduces the spacing of the selected frequencies within that window prior to the next iteration of a signal component transform 820. In this manner, a signal component transform 820 and the resulting frequency estimate are refined to a higher resolution with each iteration of signal component transform 820, extrema detection 850, and resolution refinement 880.

[0055] In a particular embodiment, the component calculation requires three iterations. A frequency resolution of 4 beats per minute or 4 BPM is used initially and a window of five or seven selected frequencies, including that of the initial pulse rate estimate PR, is defined. That is, a window of either 16 BPM or 24 BPM centered on PR is defined, and a signal component transform is computed for a set of 5 or 7 selected frequencies evenly spaced at 4 BPM. The result is a frequency estimate  $f_1$ . Next, the frequency resolution is reduced from 4 BPM to 2 BPM and a 4 BPM window centered on  $f_1$  is defined with three selected frequencies, i.e.  $f_1-2$  BPM,  $f_1$ , and  $f_1+2$  BPM. The result is a higher resolution frequency estimate  $f_2$ . On the final iteration, the frequency resolution is reduced to 1 BPM and a 2 BPM window centered on  $f_2$  is defined with three selected frequencies, i.e.  $f_2-1$  BPM,  $f_2$ , and  $f_2+1$  BPM. The final result is the component frequency  $f_o$  determined by a signal component transform to within a 1 BPM resolution. This component frequency  $f_o$  is then used to calculate the oxygen saturation,  $SAT_{f_o}$ , as described above.

[0056] The signal component processor has been described above with respect to pulse oximetry and oxygen saturation measurements based upon a frequency component that optimizes signal energy. The signal component processor, however, is applicable to other physiological measurements, such as blood glucose, carboxy-hemoglobin, respiration rate and blood pressure to name a few. Further, the signal component processor is generally applicable to identifying, selecting and processing any basis function signal components, of which single frequency components are one embodiment, as described in further detail with respect to FIG. 9, below.

[0057] FIGS. 9-11 illustrate another embodiment of a signal component processor 900. As shown in FIG. 9, the processor 900 has an index calculator 910 and a measurement calculator 960. The index calculator has a sensor signal input S 902 and outputs a basis function index  $\kappa_o$  912, as described with respect to FIG. 10, below. The measurement calculator

960 inputs the basis function index  $\kappa_o$  912 and outputs a physiological measurement  $U_{\kappa_o}$  962, as described with respect to FIG. 11, below. The processor 900 also has a basis function indicator 980, which is responsive to the sensor signal input S 902 and provides a parameter  $\epsilon$  982 that indicates a set of basis functions to be utilized by the index calculator 910, as described with respect to FIG. 10, below.

[0058] As shown in FIG. 10, the functions of the index calculator 910 are basis subset generation 1020, component cancellation 1040 and optimization calculation 1060. The basis subset generation 1020 outputs a subset  $\phi_{\kappa}$  1022 of basis function waveforms corresponding to a set of selected basis function indices  $\kappa$ . The basis functions can be any complete set of functions such that

$$S = \sum_{\kappa} a_{\kappa} \Phi_{\kappa} \quad (13)$$

[0059] For simplicity of illustration purposes, these basis functions are assumed to be orthogonal

$$\langle \vec{\phi}_{\gamma}, \vec{\phi}_{\eta} \rangle = 0; \gamma \neq \eta \quad (14)$$

[0060] where  $\langle \rangle$  denotes an inner product. As such

$$\alpha_{\kappa} = \langle S, \Phi_{\kappa} \rangle = \langle \Phi_{\kappa}, \Phi_{\kappa} \rangle = \quad (15)$$

$$S_{\kappa} = \alpha_{\kappa} \Phi_{\kappa} \quad (16)$$

[0061] In general, the basis functions may be non-orthogonal. The subset of basis functions generated is determined by an input parameter  $\epsilon$  982. In the embodiment described with respect to FIG. 5, above, the basis functions are sinusoids, the indices are the sinusoid frequencies and the input parameter  $\epsilon$  982 is a pulse rate estimate that determines a frequency window.

[0062] As shown in FIG. 10, the component cancellation 1040 generates a remainder output  $R_{\kappa}$  1042, which is a set of remainder signals corresponding to the subset of basis function waveforms  $\phi_{\kappa}$  1022. For each basis function waveform generated, component cancellation removes the corresponding basis function component from the sensor signal S 902 to generate a remainder signal. In an alternative embodiment, component cancellation 1040 is replaced with a component selection that generates a corresponding basis function component of the sensor signal S 902 for each basis function generated. The optimization calculation 1060 generates a particular index  $\kappa_o$  912 associated with an optimization of the remainders  $R_{\kappa}$  1042 or, alternatively, an optimization of the selected basis function signal components.

[0063] As shown in FIG. 11, the functions of the measurement calculator 960 are basis function generation 1120, component selection 1140, and physiological measurement calculation 1170. The component selection 1140 inputs the sensor signal S 902 and a particular basis function waveform  $\phi_{\kappa_o}$  1122 and outputs a sensor signal component  $S_{\kappa_o}$  1142. The physiological measurement 1170 inputs the sensor signal component  $S_{\kappa_o}$  1142 and outputs the physiological measurement  $U_{\kappa_o}$  962, which is responsive to the sensor signal component  $S_{\kappa_o}$  1142. In the embodiment described with respect to FIG. 6, above, the basis functions  $\phi_{\kappa}$  are sinusoids and the index  $\kappa_o$  is a particular sinusoid frequency. The basis function generation 1120 creates sine and cosine waveforms at this frequency. The component selection 1140 selects corresponding frequency components of the sensor signal por-

tions, RD and IR. Also, the physiological measurement **1170** computes an oxygen saturation based upon a magnitude ratio of these RD and IR frequency components.

**[0064]** The signal component processor has been disclosed in detail in connection with various embodiments. These embodiments are disclosed by way of examples only and are not to limit the scope of the claims that follow. One of ordinary skill in the art will appreciate many variations and modifications.

What is claimed is:

**1.** In a patient monitor configured to obtain signals responsive to physiological parameters of a monitored patient, a method for filtering one or more of said signals to improve a determination of a pulse rate of the monitored patient, the method comprising:

receiving one or more signals indicative of light attenuated by body tissue of pulsing blood in said monitored patient, said one or more signals usable to determine physiological measurements and a pulse rate of said monitored patient;

electronically determining an initial frequency estimate of said pulse rate;

electronically combining at least one sinusoidal waveform with said one or more of said signals to produce a pre-determined signal response; and

electronically processing the combined signal to determine an output measurement of said pulse rate.

**2.** The method of claim **1**, comprising sending said output measurement to a display.

**3.** The method of claim **2**, comprising displaying said output measurement.

**4.** The method of claim **1**, comprising generating one or more sinusoidal waves as the at least one sinusoidal waveform.

**5.** The method of claim **4**, comprising individually canceling the generated sinusoidal waves from the one or more signals.

**6.** The method of claim **1**, wherein said signal component processing includes determining a frequency corresponding to the sinusoidal waveform which produces an extrema.

**7.** The method of claim **1**, comprising segmenting the signal into at least one pulse rate cycle.

**8.** The method of claim **6**, wherein the extrema comprises a minima.

**9.** The method of claim **1**, wherein said signal component processing includes determining an oxygen saturation.

\* \* \* \* \*

专利名称(译)	正弦饱和变换		
公开(公告)号	<a href="#">US20090099429A1</a>	公开(公告)日	2009-04-16
申请号	US12/336419	申请日	2008-12-16
[标]申请(专利权)人(译)	梅西莫股份有限公司		
申请(专利权)人(译)	Masimo公司		
当前申请(专利权)人(译)	摩根大通银行，NATIONAL ASSOCIATION		
[标]发明人	WEBER WALTER M AL ALI AMMAR CAZZOLI LORENZO		
发明人	WEBER, WALTER M. AL-ALI, AMMAR CAZZOLI, LORENZO		
IPC分类号	A61B5/1455 G01R29/00 A61B5/02 A61B5/00 A61B5/145		
CPC分类号	A61B5/024 A61B5/14551 A61B5/1455 A61B5/14532 A61B5/14552 A61B5/02433 A61B5/7282		
优先权	60/302438 2001-06-29 US		
其他公开文献	US7904132		
外部链接	<a href="#">Espacenet</a> <a href="#">USPTO</a>		

#### 摘要(译)

公开了一种用于确定生理测量的变换。变换根据通过生理传感器获得的生理信号确定基函数指数。基于基函数索引生成基函数波形。然后使用基函数波形来确定优化的基函数波形。优化的基函数波形用于计算生理测量。

